

Wavelet Transform Based Technique for Fault Detection and Classification in a 400 kV Double Circuit Transmission Line

Neha Gautam¹, Gaurav Kapoor² and Shoyab Ali³

^{1&3}Department of Electrical Engineering, Vedant College of Engineering and Technology, Bundi, Rajasthan, India

²Department of Electrical Engineering, Modi Institute of Technology, Kota, Rajasthan, India

E-Mail: nehaeee91@gmail.com, gaurav.kapoor019@gmail.com, ali.shoyab@gmail.com

(Received 21 September 2018; Revised 17 October 2018; Accepted 31 October 2018; Available online 6 November 2018)

Abstract - This work proposes a wavelet transform based fault detection and classification technique for the protection of double circuit transmission line. The three phase current signals of both circuits recorded at Bus-1 of the double circuit transmission line power system are used to evaluate the approximate and high frequency detail coefficients at level-1. The proposed scheme is extensively tested using the test system of a 400 kV, 50 Hz double circuit transmission line simulated in MATLAB. The probability of wavelet transform based proposed technique is tested under a extensive deviation of fault parameters, such as fault location, fault type, fault inception time, fault resistance and ground resistance. The test results exemplifies that all types of faults are appropriately detected/ classified.

Keywords: Double Circuit Transmission Line Protection, Fault Detection, Fault Classification, Faulty Phase Identification, Wavelet Transform

I. INTRODUCTION

Double circuit transmission line faults have to be detected and located speedily with accuracy to facilitate the repair of faulted part, restore electricity supply and decrease outage instance as soon as feasible. Many schemes of fault detection and classification have been studied and developed over the years for the protection of double circuit transmission line. The analysis of some papers has been discussed in this segment. Recently, in [1], discrete wavelet transform has been used for the protection of low voltage DC micro-grid. In [2], wavelet transform based fault detection and faulty phase identification technique has been proposed for the protection of double circuit transmission line. In [3], mathematical morphology based fault detector has been proposed for the detection of faults in double circuit transmission line. S-transform has been used in [4] for the distance protection of STATCOM compensated three phase transmission line. In [5], artificial neural network is used for double circuit transmission line protection. Support vector machine based fault detection and classification technique has been implemented for fault detection and classification in three phase transmission line [6]. In [7], investigation of transient recovery voltage has been done across the circuit breaker of series compensated double circuit ultra high voltage transmission line. In [8], artificial neural network based phase to phase fault detection, classification and fault distance location scheme has been proposed for double circuit transmission line. Discrete wavelet transform in combination with artificial

neural network has been used in [9] for parallel transmission line protection. In [10], a sampling method based protection technique has been discussed for the protection of series compensated transmission line.

In this work, a single ended fault detection/classification method based on wavelet transform is proposed for the protection of double circuit transmission line. The paper is organized as follows: the specifications of double circuit transmission line are presented in section II. Feature extraction procedure, based on daubechies-4 wavelet, from the current signals of both circuits is discussed in section III. Section IV is dedicated to the discussion of simulation results. Finally the conclusions of the work are given in section V.

II. DOUBLE CIRCUIT TRANSMISSION LINE SPECIFICATIONS

The single line diagram of double circuit transmission line test system under study is exemplified in Fig.1. The system consists of a 400 kV, 50 Hz double circuit transmission line, bifurcated into two sections each of length 100 km. The double circuit transmission line is fed from a 400 kV source at the sending end and connected to two loads of 100 MW and 100 MVar each at the receiving end. To protect the entire double circuit transmission line, the relay is connected at bus-1 of power system as demonstrated in Fig.1. The test system is simulated using MATLAB. Daubechies-4 mother wavelet has been used for the feature extraction of fault current signals of both circuits to evaluate the approximate and detail coefficients of corresponding phase current.

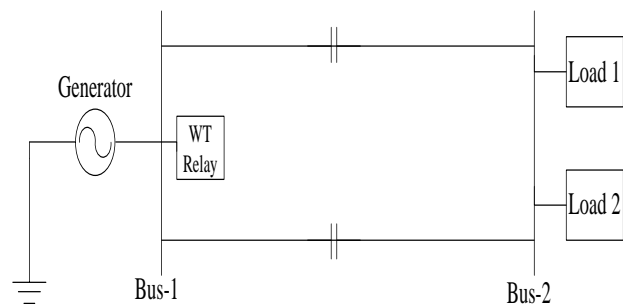


Fig. 1 Single line diagram of proposed power system

III. WAVELET TRANSFORM BASED PROPOSED TECHNIQUE

In the proposed work, fault current signals of both circuits were decomposed using daubechies-4 wavelet. Approximate coefficients can be computed for any function $f(t)$ using equation-1:

$$A_{j,k} = \langle f(t), \Phi_{j,k}(t) \rangle = \int f(t) \Phi_{j,k}(t) dt \quad (1)$$

Similarly, for any function $f(t)$ the detailed coefficients are computed using equation-2:

$$D_{j,k} = \langle f(t), \psi_{j,k}(t) \rangle = \int f(t) \psi_{j,k}(t) dt \quad (2)$$

where, j is the resolution level, and the scale function $\Phi_{j,k}(t)$ and the wavelet function $\psi_{j,k}(t)$ are determined by the mother wavelet $\psi_{a,b}$ selected.

The various steps of the proposed technique which is exemplified in Fig.2 are described in detail henceforward.

Step 1: Simulate the power system for different fault types and generate post fault three phase current signals of both circuits.

Step 2: Decompose the three phase current waveforms of both circuits using wavelet transform for feature extraction.

Step 3: Compute the magnitude of wavelet energy for each fault current signal.

Step 4: Evaluate the approximate and detail coefficients of fault current signals at level-1 using equations 1 and 2.

Step 5: If the magnitude of detail coefficients of the faulted phase is greater than the magnitude of detail coefficients of healthy phase, then fault else no fault, go to step 1.

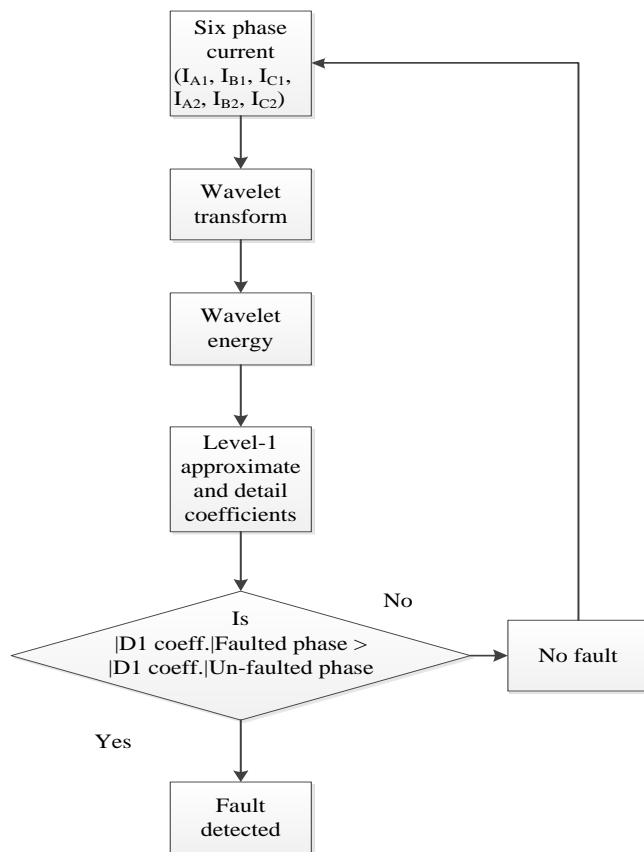


Fig. 2 Proposed fault detection and classification technique

IV. SIMULATION RESULTS AND DISCUSSIONS

The performance of the proposed technique has been evaluated for different types of fault cases. The performance has been evaluated by varying fault parameters viz. fault type, fault location, fault inception time, fault resistance and ground resistance. Test results of the proposed work are discussed in the subsequent subsections.

A. Performance during Fault Resistance Variation

The performance of the proposed fault detection technique is evaluated for faults with fault resistance variation. The three phase current of circuit-1 and circuit-2 during single line to ground fault on phase ‘A1’ of circuit-1 at 50% away from bus-1 at FIT=0.1 seconds with $R_f = 0.001 \Omega$ and $R_g = 0.001 \Omega$ is shown in Fig.3. The approximate-1 and detail-1 coefficients of three phase current of circuit-1 and circuit-2 during phase-‘A1-g’ fault are demonstrated in Figures 4-7. From the simulation result as depicted in Table I, it can be seen that the proposed technique suitably detects the fault and identifies the faulty phase and is found immune to the variation in fault resistance.

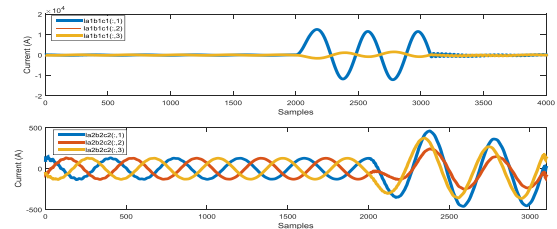


Fig. 3 Three phase current of circuit-1 and circuit-2 during phase-‘A1-g’ fault at 50% from relaying point at FIT=0.1 seconds with $R_f = 0.001 \Omega$ and $R_g = 0.001 \Omega$

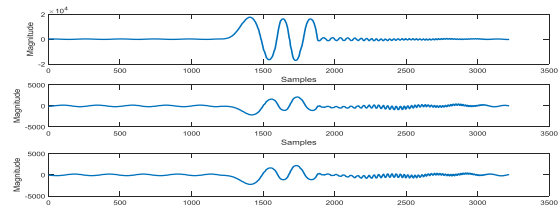


Fig. 4 Approximate-1 coefficient of three phase current of circuit-1 during phase- ‘A1-g’ fault at 50% from relaying point at FIT=0.1 seconds with $R_f = 0.001 \Omega$ and $R_g = 0.001 \Omega$

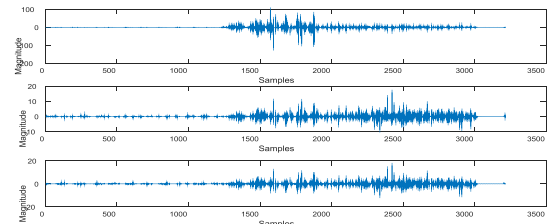


Fig.5 Detail-1 coefficient of three phase current of circuit-1 during phase- ‘A1-g’ fault at 50% from relaying point at FIT=0.1 seconds with $R_f = 0.001 \Omega$ and $R_g = 0.001 \Omega$

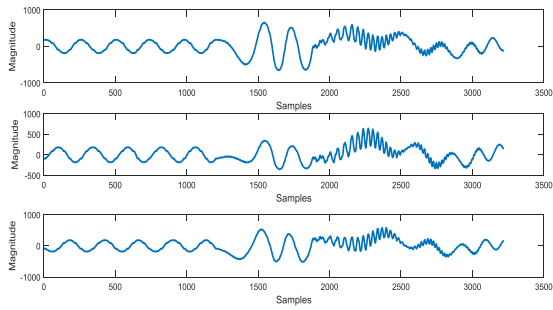


Fig.6 Approximate-1 coefficient of three phase current of circuit-2 during phase- 'A1-g' fault at 50% from relaying point at FIT=0.1 seconds with $R_f = 0.001\Omega$ and $R_g = 0.001\Omega$

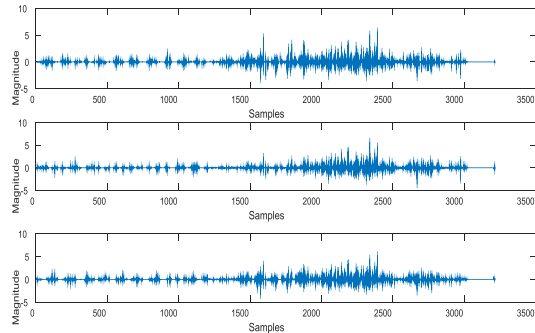


Fig.7 Detail-1 coefficient of three phase current of circuit-2 during phase- 'A1-g' fault at 50% from relaying point at FIT=0.1 seconds with $R_f = 0.001\Omega$ and $R_g = 0.001\Omega$

TABLE I TEST RESULTS OF WT FOR PHASE- 'A1-G' FAULT AT 50% FROM RELAY LOCATION AT FIT=0.1 SECONDS WITH $R_f = 0.001\Omega$ AND $R_g = 0.001\Omega$

Phase	Output		
	Approx. Coefficient	Detail Coefficient	Wavelet Energy
A1	1.7710×10^4	96.0220	99.8651
B1	2.1346×10^3	15.8607	97.4382
C1	2.1851×10^3	15.9035	97.6617
A2	653.5299	5.6774	98.2879
B2	637.2156	5.7832	96.9012
C2	574.9199	5.2567	97.7444

B. Performance during Ground Resistance Variation

The performance of the proposed technique is evaluated for faults with ground resistance variation. The three phase current of circuit-1 and circuit-2 during single line to ground fault on phase 'B1' of circuit-1 triggered at 50% away from the relaying point with $R_g = 5 \Omega$, $R_f = 0.001 \Omega$ at FIT = 0.15 seconds is demonstrated in Fig.8. The approximate-1 and detail-1 coefficients of three phase current of circuit-1 and circuit-2 for phase-'B1-g' fault are exemplified in Figures 9-12. From the simulation result as depicted in Table II, it is observed that the proposed method is not affected by ground resistance variation and effectively detects the fault with faulty phase identification.

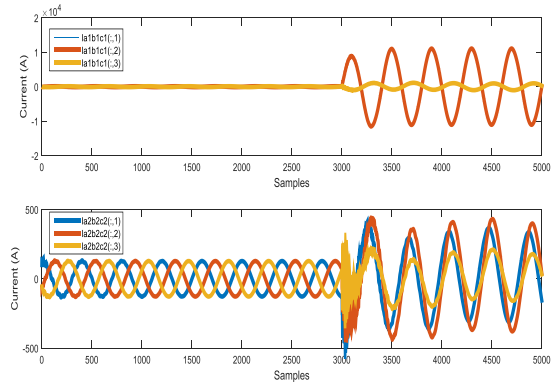


Fig. 8 Three phase current of circuit-1 and circuit-2 during phase- 'B1-g' fault at 50% from relaying point with $R_g = 5\Omega$, $R_f = 0.001\Omega$ at FIT = 0.15 seconds

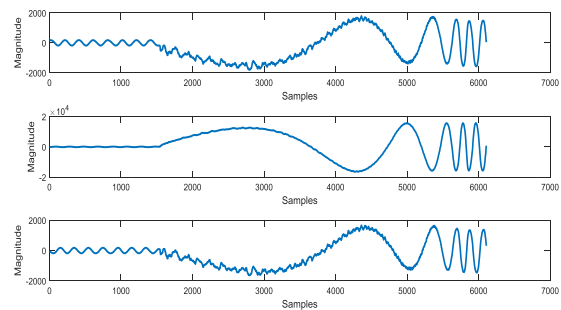


Fig. 9 Approximate-1 coefficient of three phase current of circuit-1 during phase- 'B1-g' fault at 50% from relaying point with $R_g = 5\Omega$, $R_f = 0.001\Omega$ at FIT = 0.15 seconds

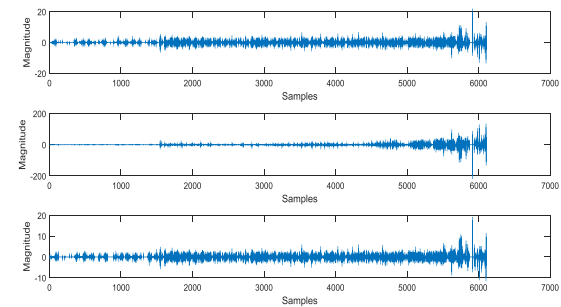


Fig. 10 Detail-1 coefficient of three phase current of circuit-1 during phase- 'B1-g' fault at 50% from relaying point with $R_g = 5\Omega$, $R_f = 0.001\Omega$ at FIT = 0.15 seconds

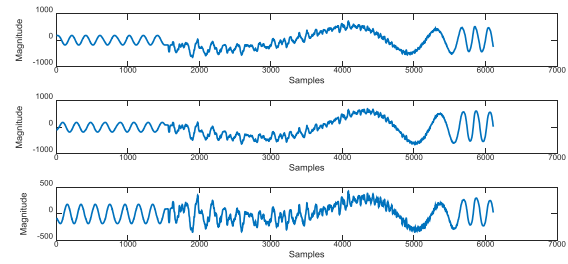


Fig. 11 Approximate-1 coefficient of three phase current of circuit-2 during phase- 'B1-g' fault at 50% from relaying point with $R_g = 5\Omega$, $R_f = 0.001\Omega$ at FIT = 0.15 seconds

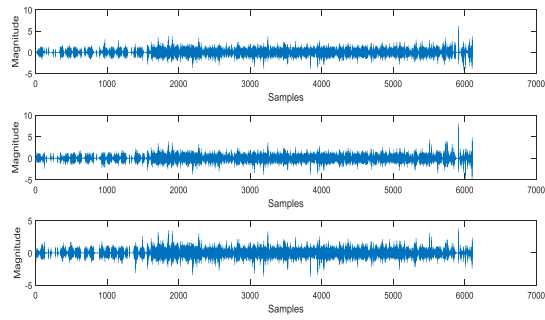


Fig. 12 Detail-1 coefficient of three phase current of circuit-2 during phase-‘B1-g’ fault at 50% from relaying point with $R_g = 5\Omega$, $R_f = 0.001\Omega$ at FIT = 0.15 seconds

TABLE II TEST RESULTS OF WT FOR PHASE-‘B1-G’ FAULT AT 50% FROM RELAY LOCATION WITH $R_g = 5\Omega$, $R_f = 0.001\Omega$ AT FIT = 0.15 SECONDS

Phase	Output		
	Approx. Coefficient	Detail Coefficient	Wavelet Energy
A1	$1.7831 \cdot 10^3$	19.6548	99.9470
B1	$1.5662 \cdot 10^4$	112.4044	99.9942
C1	$1.6539 \cdot 10^3$	17.5267	99.9352
A2	726.4401	5.3266	99.6813
B2	698.3722	7.1454	99.7360
C2	427.1992	3.1984	98.9673

C. Performance during Fault Inception Time Variation

The performance of proposed technique has been tested for faults with variation in fault inception time. The three phase current of circuit-1 and circuit-2 during phase-‘A1C1A2C2-g’ fault at 50% away from bus-1 at FIT= 0.014 seconds, $R_g = 5\Omega$ and $R_f = 2\Omega$ is shown in Fig.13. The approximate-1 and detail-1 coefficients of three phase current of circuit-1 and circuit-2 for phase-‘A1C1A2C2-g’ fault are demonstrated in Figures 14-17. Table III presents the simulation result related to the fault case simulated at 50% with fault resistance of 5Ω at FIT=0.014 seconds for phase-‘A1C1A2C2-g’ fault, respectively. The simulation result follows the exemption of the proposed fault detection and identification technique to variation in fault inception time.

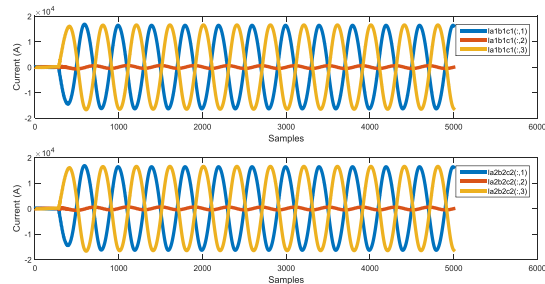


Fig. 13 Three phase current of circuit-1 and circuit-2 during phase-‘A1C1A2C2-g’ fault at 50% from relaying point at FIT= 0.014 seconds, $R_g = 5\Omega$ and $R_f = 2\Omega$

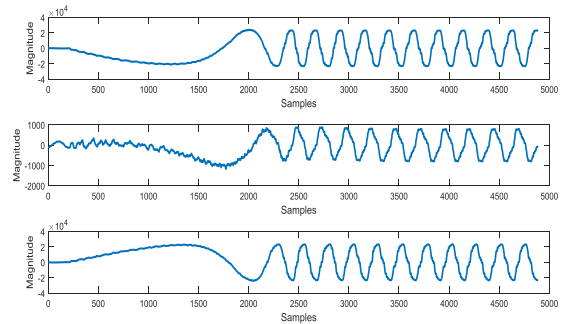


Fig. 14 Approximate-1 coefficient of three phase current of circuit-1 during phase-‘A1C1A2C2-g’ fault at 50% from relaying point at FIT=0.014 seconds, $R_g = 5\Omega$ and $R_f = 2\Omega$

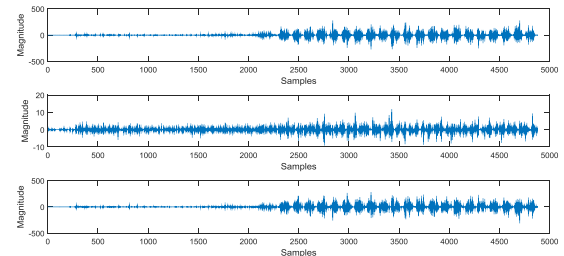


Fig. 15 Detail-1 coefficient of three phase current of circuit-1 during phase-‘A1C1A2C2-g’ fault at 50% from relaying point at FIT=0.014 seconds, $R_g = 5\Omega$ and $R_f = 2\Omega$

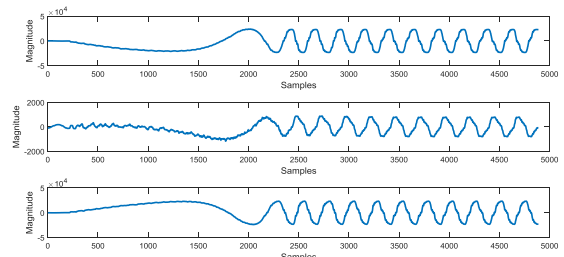


Fig. 16 Approximate-1 coefficient of three phase current of circuit-2 during phase-‘A1C1A2C2-g’ fault at 50% from relaying point at FIT=0.014 seconds, $R_g = 5\Omega$ and $R_f = 2\Omega$

TABLE III TEST RESULTS OF WT FOR PHASE-‘A1C1A2C2-G’ FAULT AT 50% FROM RELAY LOCATION AT FIT= 0.014 SECONDS, $R_g = 5\Omega$ AND $R_f = 2\Omega$

Phase	Output		
	Approx. Coefficient	Detail Coefficient	Wavelet Energy
A1	$2.3966 \cdot 10^4$	222.4978	99.8486
B1	876.7508	10.1305	99.7250
C1	$2.3363 \cdot 10^4$	224.8065	99.8167
A2	$2.3966 \cdot 10^4$	222.4978	99.8486
B2	876.7508	10.1305	99.7250
C2	$2.3363 \cdot 10^4$	224.8065	99.8167

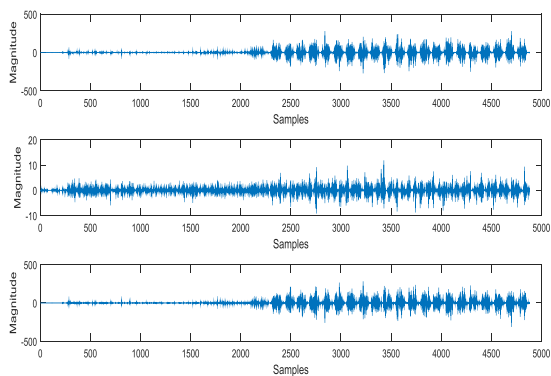


Fig. 17 Detail-1 coefficient of three phase current of circuit-2 during phase- ‘A1C1A2C2-g’ fault at 50% from relaying point at FIT=0.014 seconds, $R_g = 5\Omega$ and $R_f = 2\Omega$

D. Performance during Close-in Fault

It is very important to estimate the performance of any fault detection method for a close-in fault. The relay should operate appropriately for a close-in fault and it should exactly identify the faulty phases. Thus, the performance of the proposed scheme is examined during phase- ‘A2B2C2-g’ fault at 5% from bus-1 with $R_f = 50 \Omega$, $R_g = 30 \Omega$ at FIT=0.1 seconds. The three phase current of circuit-1 and circuit-2 during phase- ‘A2B2C2-g’ fault at 5% away from relaying point with $R_f = 50 \Omega$, $R_g = 30 \Omega$ at FIT=0.1 seconds is demonstrated in Fig.18. The approximate-1 and detail-1 coefficients of three phase current of circuit-1 and circuit-2 during phase- ‘A2B2C2-g’ fault at 5% from the relay location are exemplified in Figures 19-22. Further, Table IV shows the output of the fault detector for phase- ‘A2B2C2-g’ fault triggered at 5%. It can be concluded that the fault detector correctly detects the near-end fault and identifies the faulty phase accurately with 100% accurateness.

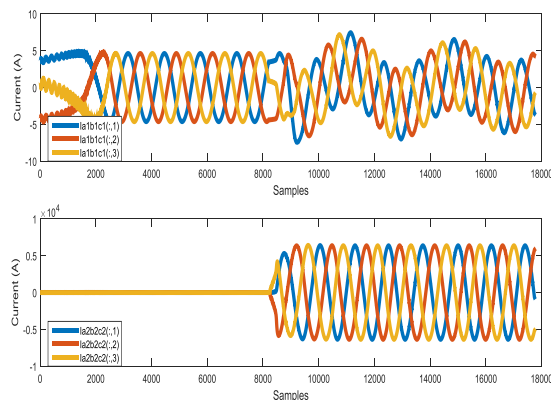


Fig. 18 Three phase current of circuit-1 and circuit-2 during phase- ‘A2B2C2-g’ fault at 5% from relaying point with $R_f = 50\Omega$, $R_g = 30\Omega$ at FIT=0.1 seconds

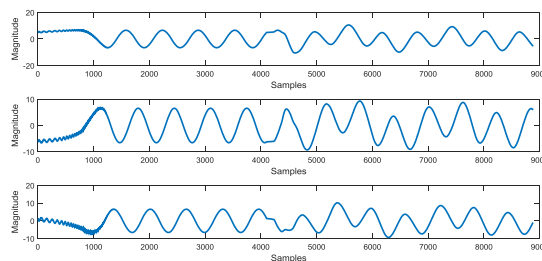


Fig. 19 Approximate-1 coefficient of three phase current of circuit-1 during phase- ‘A2B2C2-g’ fault at 5% from relaying point with $R_f = 50\Omega$, $R_g = 30\Omega$ at FIT=0.1 seconds

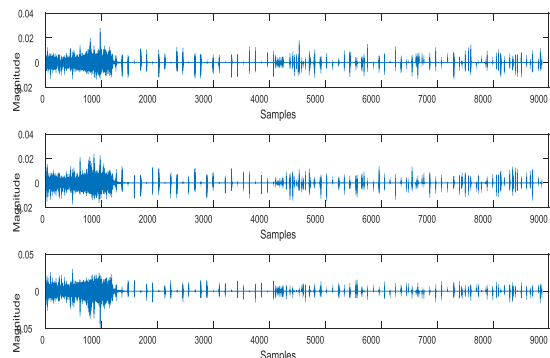


Fig. 20 Detail-1 coefficient of three phase current of circuit-1 during phase- ‘A2B2C2-g’ fault at 5% from relaying point with $R_f = 50\Omega$, $R_g = 30\Omega$ at FIT=0.1 seconds

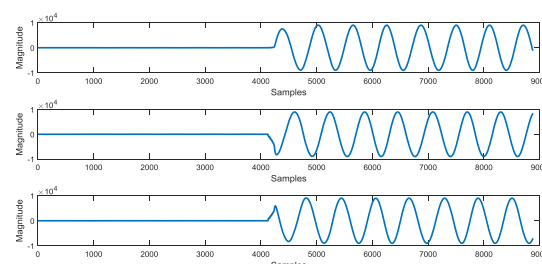


Fig. 21 Approximate-1 coefficient of three phase current of circuit-2 during phase- ‘A2B2C2-g’ fault at 5% from relaying point with $R_f = 50\Omega$, $R_g = 30\Omega$ at FIT=0.1 seconds

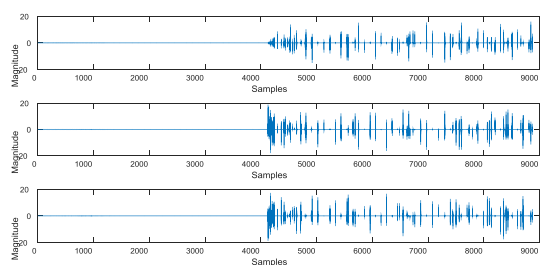


Fig. 22 Detail-1 coefficient of three phase current of circuit-2 during phase- ‘A2B2C2-g’ fault at 5% from relaying point with $R_f = 50\Omega$, $R_g = 30\Omega$ at FIT=0.1 seconds

TABLE IV TEST RESULTS OF WT FOR PHASE-‘A2B2C2-G’ FAULT AT 5% FROM RELAY LOCATION WITH $R_f = 50\Omega$, $R_g = 30\Omega$ AT FIT=0.1 SECONDS

Phase	Output		
	Approx. Coefficient	Detail Coefficient	Wavelet Energy
A1	10.5385	0.0245	99.9930
B1	9.2882	0.0203	99.9876
C1	10.1672	0.0243	99.9570
A2	9.0258×10^3	13.7120	99.9997
B2	9.0023×10^3	16.5370	99.9990
C2	9.0602×10^3	15.0048	99.9992

E. Performance during Far-end Fault

It is very noteworthy to evaluate the performance of any fault detection technique for remote-end faults because there is a probability of the relay to under reach during a remote-end fault. The fault detector should operate correctly for a remote-end fault and should correctly classify the faulty phases. To estimate the performance of the proposed fault detection technique under this type of circumstance, a two phase to ground fault phase-‘A1C1-g’ fault at 90% away from bus-1 with $R_f = 0.5 \Omega$, $R_g = 1 \Omega$ and at FIT=0.2 seconds is simulated, and the simulation result is illustrated in Fig.23. The approximate-1 and detail-1 coefficients of three phase current of circuit-1 and circuit-2 during phase-‘A1C1-g’ fault at 90% away from relay location are shown in Figures 24-27. Further, Table V shows the output of relay for phase-‘A1C1-g’ fault at 90% from bus-1.

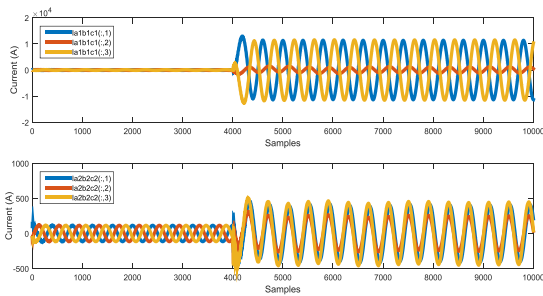


Fig. 23 Three phase current of circuit-1 and circuit-2 during phase-‘A1C1-g’ fault at 90% from relaying point with $R_f = 0.5\Omega$, $R_g = 1\Omega$ at FIT=0.2 seconds

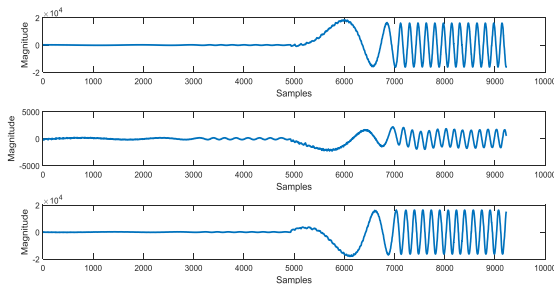


Fig. 24 Approximate-1 coefficient of three phase current of circuit-1 during phase- ‘A1C1-g’ fault at 90% from relaying point with $R_f = 0.5\Omega$, $R_g = 1\Omega$ at FIT=0.2 seconds

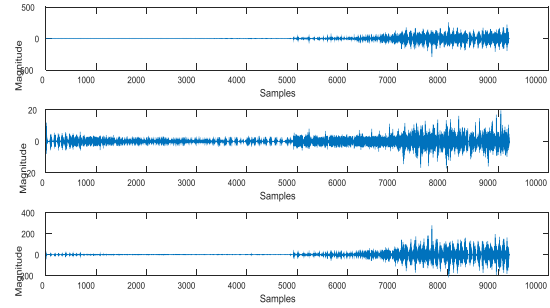


Fig. 25 Detail-1 coefficient of three phase current of circuit-1 during phase- ‘A1C1-g’ fault at 90% from relaying point with $R_f = 0.5\Omega$, $R_g = 1\Omega$ at FIT=0.2 seconds

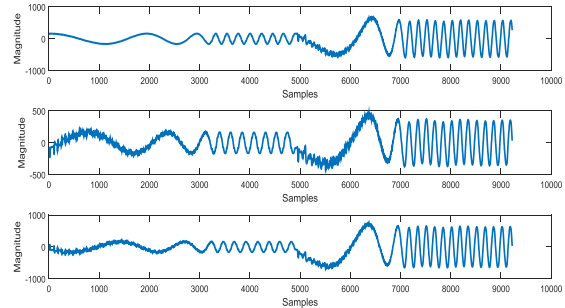


Fig. 26 Approximate-1 coefficient of three phase current of circuit-2 during phase- ‘A1C1-g’ fault at 90% from relaying point with $R_f = 0.5\Omega$, $R_g = 1\Omega$ at FIT=0.2 seconds

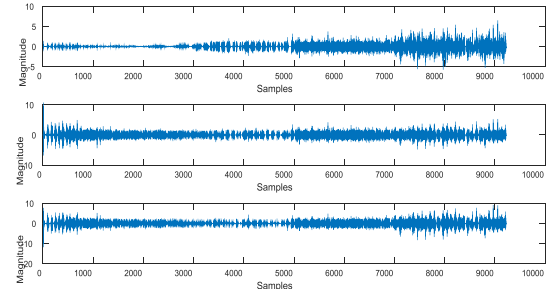


Fig. 27 Detail-1 coefficient of three phase current of circuit-2 during phase- ‘A1C1-g’ fault at 90% from relaying point with $R_f = 0.5\Omega$, $R_g = 1\Omega$ at FIT=0.2 seconds

TABLE V TEST RESULTS OF WT FOR PHASE-‘A1C1-G’ FAULT AT 90% FROM RELAY LOCATION WITH $R_f = 0.5\Omega$, $R_g = 1\Omega$ AT FIT=0.2 SECONDS

Phase	Output		
	Approx. Coefficient	Detail Coefficient	Wavelet Energy
A1	1.8468×10^4	202.0114	99.9625
B1	2.1601×10^3	17.4385	99.9362
C1	1.6315×10^4	245.1416	99.9614
A2	686.7171	5.6486	99.8456
B2	480.4296	9.5915	99.4737
C2	758.1146	7.4223	99.7813

V. CONCLUSION

Wavelet transform based fault detection and classification technique for double circuit transmission line protection is found to be extremely successful under various fault conditions. The strength of the proposed technique is not affected by different fault circumstances such as variation in fault type, fault resistance, ground resistance, fault location and fault inception time. Test results exemplifies that the proposed scheme effectively detects the fault and classifies the fault type and the faulty phase absolutely. The main advantage of using this technique is that this method uses the samples of three phase currents of both the circuits recorded at particular end only i.e. at bus-1 of a proposed power system.

REFERENCES

- [1] S. Som and S. R. Samantaray, "Efficient protection scheme for low-voltage DC micro-grid", *IET Generation, Transmission, and Distribution*, Vol. 12, No. 13, pp. 3322-3329, 2018.
- [2] N. Gautam, S. Ali and G. Kapoor, "Detection of fault in series capacitor compensated double circuit transmission line using wavelet transform", *Proc. IEEE Int. Conf. Computing, Power and Communication Technologies (GUCON)*, pp. 769-773, 2018.
- [3] G. Kapoor, "Mathematical morphology based fault detector for protection of double circuit transmission line", *ICTACT J. of Microelectronics*, Vol. 4, No. 2, pp. 589-600, 2018.
- [4] P. K. Dash, S. Das and J. Moirangthem, "Distance protection of shunt compensated transmission line using a sparse S-transform", *IET Generation, Transmission, and Distribution*, Vol. 9, No. 12, pp. 1264-1274, 2015.
- [5] A. Yadav and A. Swetapadma, "Improved first zone reach setting of artificial neural network-based directional relay for protection of double circuit transmission lines", *IET Gener., Transm. Distrib.*, Vol. 8, No. 3, pp. 373-388, 2014.
- [6] A. A. Yusuff, A. A. Jimoh and J.L. Munda, "Determinant-based feature extraction for fault detection and classification for power transmission lines", *IET Generation, Transmission, and Distribution*, Vol. 5, No. 12, pp. 1259-1267, 2011.
- [7] Zutao Xiang, Jiming Lin, Liangeng Ban, and Bin Zheng, "Investigation of TRV across Circuit Breaker of Series Compensated Double-Circuit UHV Transmission Lines", *Proc. IEEE-Power Con.*, pp. 1-5, October 2010.
- [8] A. Jain, A. S. Thoke, E. Koley, and R. N. Patel, "Fault Classification and Fault Distance Location of Double Circuit Transmission Lines for Phase to Phase Faults using only One Terminal Data", *Proc. IEEE Int. Conf. Power System*, pp. 1-6, 2009.
- [9] A. Swetapadma and A. Yadav, "Time Domain Complete Protection Scheme for Parallel Transmission Lines", *Ain Shams Engineering J.*, Vol. 7, No. 1, pp. 169-183, 2016.
- [10] P. Jafarian and M. S. Pasand, "High-Speed Superimposed based Protection of Series-Compensated Transmission Lines", *IET Generation, Transmission, and Distribution*, Vol.-5, No.-12, pp. 1290-1300, 2011.
- [11] P. Sharma, S. Ali and G. Kapoor, "Fault detection on series capacitor compensated transmission line using Walsh hadamard transform", *Proc. IEEE Int. Conf. Computing, Power and Communication Technologies (GUCON)*, pp. 763-768, 2018.
- [12] G. Kapoor, "Fault detection of phase to phase fault in series capacitor compensated six phase transmission line using wavelet transform", *Jordan J. Electrical Engineering*, Vol. 4, No. 3, pp. 151-164, 2018.
- [13] N. Sharma, S. Ali and G. Kapoor, "Fault detection in wind farm integrated series capacitor compensated transmission line using Hilbert huang transform", *Proc. IEEE Int. Conf. Computing, Power and Communication Technologies (GUCON)*, pp. 774-778, 2018.
- [14] G. Kapoor, "Six phase transmission line boundary protection using mathematical morphology", *Proc. IEEE Int. Conf. Computing, Power and Communication Technologies (GUCON)*, pp. 857-861, 2018.
- [15] P. Sharma, S. Ali and G. Kapoor, "Wavelet transform approach for fault detection of three phase transmission line compensated with series capacitor", *Asian J. Electrical Sciences*, Vol. 7, No. 2, pp. 8-13, 2018.